PHYSICAL REVIEW D VOLUME 47, NUMBER 8 15 APRIL 1993

Ultraviolet regularization of light-cone Hamiltonian perturbation theory: Application to the anomalous magnetic moment of the electron ($g-2$) in the light-cone gauge

Alex Langnau and Matthias Burkardt*
Stanford Linear Accelerator Center, Stanford University, Stanford, California 94309
(Received 23 April 1992)

An ultraviolet regularization and renormalization procedure of light-cone perturbation theory which is suitable for a numerical application is discussed. The fourth-order correction to the anomalous magnetic moment of the electron in the light-cone gauge is computed. Several regularizations of the associated light-cone gauge singularity are explored. Local counterterms are constructed to remove the quadratic light-cone divergences from the formalism. Problems of discrete light-cone quantization (DLCQ), beyond one-photon exchange, are also described.

PACS number(s): 11.10.Gh

I. INTRODUCTION

Perhaps the most outstanding problem of light-cone quantization is to compute the bound-state spectrum and relativistic wave functions of hadrons at strong coupling. In quantum chromodynamics (QCD) one needs a practical computational method which not only determines the hadronic spectra, but also provides nonperturbative hadronic matrix elements [1].

In addition, it is particularly important to compute the relativistic wave functions needed to calculate structure functions, form factors, and other hadronic matrix elements. The computation of parton distributions is perhaps among the most interesting applications of light-cone quantization since these distributions are related to the Fourier transform of correlation functions along a lightlike direction. Thus, parton distributions are "kinematic" observables given the equal light-cone time wave function.

A step in this direction has been undertaken by a method known as discrete light-cone quantization (DLCQ). So far, the theory has been applied mainly to the elucidation of quantum field theories in one space and one time dimension. In $(1+1)$-dimensional QCD, for example, the full spectra and wave functions could be obtained using the DLCQ method [2]. These results, which required only a minimal numerical effort, are in agreement with other calculations when available. The success of DLCQ, as well as a similar approach known as the light-front Tamm-Dancoff method [3], provide hope for solving field theories in $3+1$ dimensions.

However, the transition to dimensions higher than $1+1$ is anything but straightforward. Some of the reasons are the following.

(i) Theories in $1+1$ dimensions, quantized on the light cone, are manifestly covariant. This is because the operator of certain boost transformations, which is a kinematic Poincaré operator in light-cone quantization, is the only generator of continuous Lorentz transformations. This is generally not the case in higher-dimensional field theories, since the underlying Poincaré group includes certain rotation operators, which are dynamical in the light-cone formulation. Thus, the recovery of Lorentz-invariant physical observables is a nontrivial problem in light-cone-quantized theories beyond $1+1$ dimensions (as for any form of Hamiltonian dynamics) [4].

(ii) The Hamiltonian formulation of gauge theories in $1+1$ dimensions is effectively gauge invariant [5]. However, in higher dimensions the regularization imposed in such a formalism will generally spoil gauge invariance, since the gauge-field quanta become a dynamical degree of freedom of the theory. Unless a careful regularization is imposed, gauge-invariant amplitudes are *not* recovered in the continuum limit.

(iii) Simple theories such as the Yukawa model or gauge theories in $1+1$ dimensions are superrenormalizable. In $3+1$ dimensions, however, a renormalization scheme to all orders in the coupling constant and masses must be imposed for these theories in order to ensure a consistent treatment of their short-distance behavior.

(iv) The number of degrees of freedom in $(3+1)$-dimensional theories is drastically enhanced compared to the $(1+1)$-dimensional toy world.

Thus, a thorough investigation of light-cone properties which are characteristic for higher dimensions is very important. The easiest way of addressing these issues is by analyzing the perturbative structure of light-cone field theories first. Perturbative studies cannot be substituted for an analysis of problems related to a nonperturbative approach. However, in order to prepare for upcoming nonperturbative studies, it is important to validate the renormalization methods at the perturbative level. A clear understanding of divergences in perturbation theory, as well as their numerical treatment, is an important step in such a program [6].

One objective of this paper is to explore some of these issues in the example of the anomalous magnetic moment of the electron $a=(g-2)/2$ to order $(\alpha/\pi)^2$. In particular, the discussion shall focus on a renormalization

*Present address: Center for Theoretical Physics, Massachusetts Insitute of Technology, Cambridge, MA 02139.

scheme which is also suitable for a numerical treatment. This requires the construction of certain counterterms on the local level in order to prevent round-off errors.

The second section of this paper addresses problems associated with quadratic divergences in light-cone-quantized gauge theories. It has been shown that Feynman gauge leads to an infinite number of quadratic divergent light-cone perturbation theory (LCPT) diagrams at one loop [7]. The situation is significantly better in light-cone gauge since in the continuum only the self-energy and the vacuum polarization display a quadratic divergence at one loop. However, a computation in $A^+=0$ gauge requires a careful regularization of the associated gauge singularity. Most regulators reduce the small-x behavior of the light-cone photon propagator to that present in Feynman gauge. Thus, an understanding of Feynman gauge is essential even if calculations are carried out in $A^+=0$ gauge.

In Sec. III the fourth-order correction of $g-2$ in the light-cone gauge is computed. Two different descriptions for the regularization of the k^+ singularity are discussed. The sensitivity of physical observables to a finite truncation is investigated.

In Sec. IV ultraviolet regulators, which are commonly used for the purpose of nonperturbative calculations in DLCQ, are tested. It is shown that these regulators do not recover the correct answer for $a=(g-2)/2$ in fourth order, unless special counterterms are invoked.

II. LIGHT-CONE QUANTIZATION IN FEYNMAN GAUGE

In any gauge different from light-cone gauge, canonical light-cone quantization is anything but straightforward. This is due to the fact that, after solving the spinor constraint equation, the light-cone Hamiltonian in these gauges contains terms which are of arbitrarily high order in the A^+ field. Thus, in this case, we will not attempt to write down the light-cone Hamiltonian. However, even without constructing the light-cone Hamiltonian explicitly, one can still derive light-cone perturbation theory (LCPT) rules for Feynman gauge simply by separating the various light-cone time orderings of the Feynman amplitudes. A useful reference can be found in [8,9].

Feynman perturbation theory in Feynman gauge has the advantage that even off-shell Green's functions exhibit the full Lorentz structure. This simple feature provides important consistency checks for light-cone-quantized field theories, since manifest covariance is lost in this case. In addition, it helps to disentangle problems associated with singularities in the light-cone gauge propagator from problems intrinsic to light-cone quantization itself.

We start our discussion with the evaluation of the fourth-order correction to the anomalous magnetic moment of the electron $(g-2)/2$ in LCPT. The Feynman diagrams and the corresponding light-cone time orderings are displayed in Fig. 1. The techniques we used for this calculation have been discussed elsewhere [10] so that we only compare the LCPT answer of the anomaly,

$$a_{\mathrm{LCPT}}=(-0.324\pm0.004)\frac{\alpha^2}{\pi^2}\ ,$$

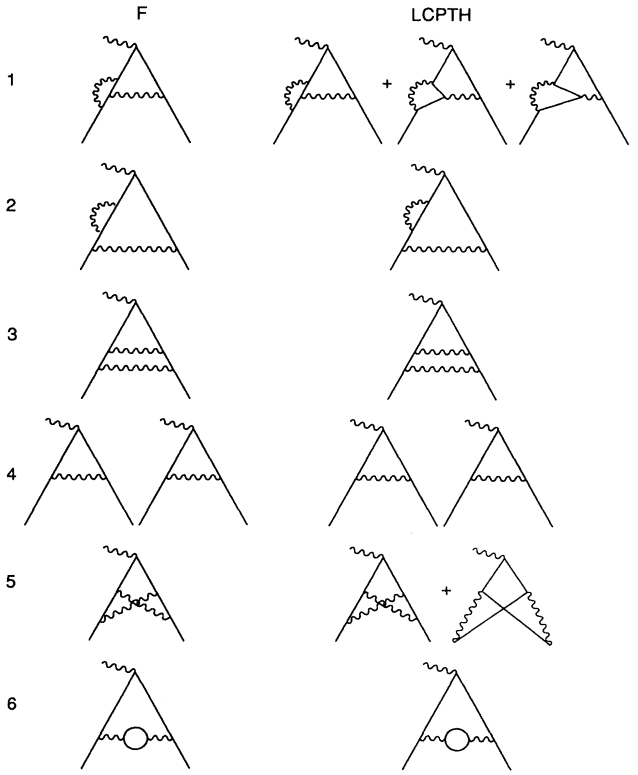

FIG. 1. Feynman diagrams F with corresponding light-cone time-ordered diagrams contributing to the electron anomalous magnetic moment $a=(g-2)/2$ to fourth order.

with the analytic result by Petermann and Sommerfield [11,12]:

$$a=-0.327\cdots\frac{\alpha^2}{\pi^2}\ .$$

Also, some sixth-order contributions have been calculated using LCPT [10].

It should be emphasized that, in order to obtain this agreement, additional renormalization, beyond usual procedures, is necessary for the self-energy diagram 2 in Fig. 1. This is because the one-loop self-energy exhibits a quadratic divergence in light-cone quantization, which is rather atypical for gauge theories [13]. The "method of alternate denominators" has been suggested as a possible solution to this problem [14]. However, in the Appendix A we show that this method must be used with caution if one wants to recover the usual Feynman answer for general perturbative processes.

Whereas the problem of the one-loop quadratically divergent self-energy occurs also in $A^+=0$ gauge, any gauge different from light-cone gauge, such as Feynman gauge, poses extra problems in light-cone quantization. To see this, we consider the "jellyfish graph" (Fig. 2) with n $(n\geq 0)$ external photons inserted into the loop. For any n we find a quadratic divergence in this diagram [15]. Furthermore, extra logarithmic divergences occur, which can be seen by power counting of the diagram in Fig. 3 [16,17].

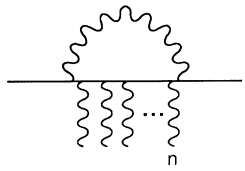

FIG. 2. n-photon jellyfish graph.

In the following we demonstrate that extra divergences in light-cone field theories can be associated with certain noncovariant terms appearing in the light-cone formalism. As an example, we investigate the $n=0$ jellyfish graph $I_{n=0}$ (which is actually just the one-loop self-energy) with momentum $p=(p^+,p^-,p_\perp)$. We leave the explicit calculation to Appendix B and quote the result obtained after mass renormalization (throughout the paper we use the notation $p^\pm=p^0\pm p^3, \gamma^\pm=\gamma^0\pm\gamma^3$):

$$I_{n=0}=(\not{p}-m)B+(\not{p}-m)^2\Sigma(p^2)+\left[\frac{\gamma^+}{p^+}-\frac{\bar{u}\gamma^+u}{2mp^+}\right]C \tag{2.1}$$

or

$$\frac{1}{4}\mathrm{tr}(\gamma^- I_{n=0})=p^-[B-2m\Sigma(p^2)]+\frac{2}{p^+}C\ . \tag{2.2}$$

In the following we want to imply that the integral $\int d\lambda^2\rho(\lambda^2)=0$ is always taken; i.e., one Pauli-Villars subtraction is assumed. In the above example we find

$$C\frac{\gamma^+}{p^+}=\frac{e^2}{16\pi^3}\frac{\gamma^+}{p^+}\int d^2k_\perp \ln\frac{m^2+k_\perp^2}{\lambda^2+k_\perp^2}\ . \tag{2.3}$$

The quadratic divergence can be identified with the term C in (2.1) and is therefore associated with the noncovariant structure in the self-energy.

We note that the occurrence of noncovariant terms of the form $C\gamma^+/p^+$ is not restricted to the one-loop self-energy (for an explicit two-loop example see Ref. [7]). In fact, all noncovariant terms we have encountered have had this structure (for a discussion of vacuum polarization contributions see [18]). As far as the self-energy is concerned, a method which is based on the correct tensor structure of the diagram can be proposed. This is possible since different tensor components should be related by covariance:

$$\mathrm{tr}(\gamma^- I_{\text{self energy}})=\frac{p^-}{p^+}\mathrm{tr}(\gamma^+ I_{\text{self energy}})\ , \tag{2.4}$$

where p^+,p^- correspond to the momentum of the fermion and $I_{\text{self energy}}$ denotes the fermion self-energy. In one loop it is straightforward to show that (2.4) is equivalent to the effective replacement

$$p_2^- \to p^-_{1\ \text{energy shell}}\frac{p_2^+}{p_1^+} \tag{2.5}$$

(see Fig. 4) in the Dirac numerator, where $p_1^+=p^+$, $p_2^+=p_1^+-k^+$, $p_{1\ \text{energy shell}}=p^-$. The momenta p^+,p^- denote the total light-cone momentum and energy, respectively. Here, k^+ is given by the light-cone momentum of the virtual photon. More generally, $p^-_{1\ \text{energy shell}}=p^--(\lambda^2+k_\perp^2)/k^+$ defines the light-cone energy one would obtain if light-cone energy conservation was imposed. The replacement (2.5) expresses the "bad component" (i.e., γ^+) in terms of the "good component" (i.e., γ^-) and thus renders the self-energy covariant by construction. Hence, the problem of the quadratic divergence is avoided in this case [19]. Equation (2.4) can be generalized to higher-loop self-energy diagrams, provided all subloops are first rendered covariant and the noncovariant piece is of the form $C\gamma^+/p^+$.

Whereas the tensor method provides a useful practical tool for dealing with the quadratic divergence in self-energy diagrams, the application of the tensor method for the cure of the jellyfish diagram with $n\geq 1$ is not straightforward. This is because the different tensor components are not simply related in this case.

It should be noted that in $3+1$ dimensions the noncovariant term in Eq. (2.2) and all other jellyfish diagrams can be eliminated more systematically if the spectral conditions [20,21]

$$\begin{aligned}&\int d\lambda^2\rho(\lambda^2)=0\ ,\\ &\int d\lambda^2\lambda^2\rho(\lambda^2)=0\ ,\\ &\int d\lambda^2\lambda^2\ln(\lambda^2)\rho(\lambda^2)=0\end{aligned} \tag{2.6}$$

are introduced. This corresponds to the introduction of three Pauli-Villars ghost particles. This is in contrast to covariant perturbation theory, where at most one Pauli-Villars (PV) photon is needed to render all jellyfish diagrams finite. Hence it is instructive to investigate the origin of these three PV conditions in light-cone quantization. In coordinate space, the one-loop self-energy is given by

$$\Sigma^{1\ \text{loop}}\sim\int d^4x\ \Delta_F(x)\gamma^\mu S_F(x)\gamma_\mu\ ,$$

where $\Delta_F(x)$ and $S_F(x)$ denote the usual boson and fermion propagators, respectively. Clearly, light-cone perturbation theory (keeping x^+ fixed while integrating out x^- and $x_\perp$ first) would give the same answer for $\Sigma^{1\ \text{loop}}$ as time-ordered perturbation theory if there were no singu-

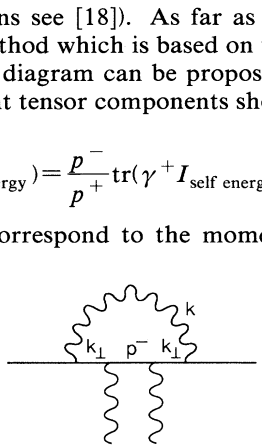

FIG. 3. Power counting for the $n=2$ jellyfish diagram leads to a logarithmic divergence.

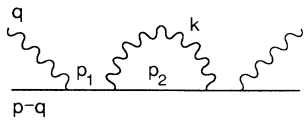

FIG. 4. One-loop correction to Compton scattering.

larity at $x^2=0$. As the leading singularity of the propagators $S_F(x)\sim x^\mu\gamma_\mu/(x^2)^2$ and $\Delta_F(x)\sim 1/x^2$ are mass independent, there are two possibilities for regulating this singularity. Either both propagators are regulated by introducing one PV photon and one PV fermion into the formalism, thereby reducing the leading singularity by two powers of x^2, or only $\Delta_F(x)$ is regulated, which has the advantage of preserving current conservation. In order to achieve the same degree of regularization in this case (reducing the singularity by two powers of x^2) one needs not only to impose the condition $\lim_{x^2\to 0}x^2\Delta_F^{\rm reg}(x^2)=0$ but also $\lim_{x^2\to 0}\Delta_F^{\rm reg}(x^2)=0$. The expansion of the boson propagator around $x^2=0$ then yields [22]

$$\Delta_F(x^2,\lambda^2)=-\frac{1}{4\pi^2}\frac{1}{x^2-i\epsilon}+\frac{\lambda^2\Theta(x^2)}{16\pi}+\frac{\lambda^2}{16\pi^2}\ln\frac{\lambda^2x^2}{4}\ ,$$

precisely condition (2.6) encountered earlier.

However, such a large number of Pauli-Villars conditions is awkward from a numerical view, since the number of degrees of freedom is enhanced dramatically in this case. For example, because of Eq. (2.6), a typical two-loop Feynman diagram, requires 16 independent computations of its integrand at each integration point. This is in contrast with only four computations in a covariant approach. In addition, the quadratic divergences would be canceled only among contributions from different Pauli-Villars particles. However, for the purpose of numerical calculations it is extremely inconvenient to cancel quadratic divergences among different diagrams because of the limited accuracy of any numerical procedure.

Hence, for practical purposes, it is necessary to develop a recipe which reduces the number of Pauli-Villars particles as well as subtracts quadratic divergences locally, i.e., before integration. In this context we shall introduce the "null subtraction" as such a local procedure. For $n=0$ the idea of the null subtraction is based on the observation that the troublesome term in Eq. (2.2) is given by

$$\frac{C}{p^+}=\frac{1}{8}\mathrm{tr}(\gamma^-I_{n=0})_{p^-=0,p_\perp=0}\ , \tag{2.7}$$

where C is independent of the external momenta. Hence, we define the null subtraction as a procedure where the "bad" component of a quadratically divergent graph or subgraph is subtracted for vanishing external (with respect to the divergent graph or subgraph) p^- and $p_\perp$ momenta, while keeping $p^+\geq 0$. In the above example we obtain for the null subtraction

$$I_{\rm null}=\frac{e^2}{16\pi^3}\int_0^1\frac{dx\,d^2k_\perp}{x(1-x)}\frac{\frac{1}{2}\gamma^\mu\frac{\gamma^+}{p^+}\frac{k_\perp^2+m^2}{1-x}\gamma_\mu}{-\frac{m^2+k_\perp^2}{1-x}-\frac{\lambda^2+k_\perp^2}{x}}\ . \tag{2.8}$$

Performing replacements similar to those given in Appendix B yields

$$I_{\rm null}=-\frac{e^2}{16\pi^3}\frac{\gamma^+}{p^+}\int_0^1dx\int d^2k_\perp\frac{\lambda^2-m^2}{k_\perp^2+\lambda^2(1-x)+m^2x} \tag{2.9}$$

$$=\frac{e^2}{16\pi^3}\frac{\gamma^+}{p^+}\int_0^1dx\int d^2k_\perp\frac{d}{dx}\ln[m^2x+\lambda^2(1-x)+k_\perp^2]=\frac{e^2}{16\pi^3}\frac{\gamma^+}{p^+}\int d^2k_\perp\ln\frac{m^2+k_\perp^2}{\lambda^2+k_\perp^2}\ .$$

What we encounter here is nothing but the noncovariant piece of Eq. (2.3). Hence, the null subtraction removes the quadratic divergence automatically in the correct way.

Let us examine now the null subtraction for the jellyfish graph for $n=1$ (which is actually the one-loop vertex correction in this case). The covariant answer is expected to be of the form [23]

$$\Gamma^\mu=\gamma^\mu F_1(q^2)+\frac{i}{2m}\sigma^{\mu\nu}q_\nu F_2(q^2)\ . \tag{2.10}$$

Using the Gordon decomposition, Eq. (2.10) can be rewritten as

$$\bar u\Gamma^+u=\bar u\gamma^+u[F_1(q^2)+F_2(q^2)]-\frac{1}{2}(p+p')^+F_2(q^2)\frac{(p+p')^+}{\sqrt{p^+p'^+}}\delta_{\lambda\lambda'}\ , \tag{2.11}$$

$$\bar u\Gamma^-u=\bar u\gamma^-u[F_1(q^2)+F_2(q^2)]-\frac{1}{2}(p+p')^-F_2(q^2)\frac{(p+p')^+}{\sqrt{p^+p'^+}}\delta_{\lambda\lambda'}\ , \tag{2.12}$$

where λ,λ' denote the initial and final helicity, respectively. The momenta p and p' correspond to the initial and final fermion, respectively. If one inserts the analytic form for the second term on the right-hand side (RHS) of Eqs. (2.11) and (2.12), the sum $F_1(q^2)+F_2(q^2)$ may be computed in two different ways: $F_1(q^2)+F_2(q^2)$ can be obtained from the Γ^+ current by means of Eq. (2.11). This is straightforward, since we do not expect trouble in this case [24,25]. However, the extraction of $F_1(q^2)+F_2(q^2)$ by means of Eq. (2.12), i.e., by computing the Γ^- current, requires a null subtraction which takes the form

$$I_{\rm null}^{(n=1)}=\frac{e^2}{16\pi^3}\int_0^1\frac{dxd^2k_\perp}{x(1-x)^2}\frac{\gamma^\mu\frac{1}{2}\gamma^+\frac{k_\perp^2+\lambda^2}{x}\gamma^-\frac{k_\perp^2+\lambda^2}{x}\frac{1}{2}\frac{\gamma^+}{p^+}\gamma_\mu}{\left[-\frac{m^2+k_\perp^2}{1-x}-\frac{\lambda^2+k_\perp^2}{x}\right]^2}\ . \tag{2.13}$$

Note that we only subtract the γ^+ component for zero external p^- and $p_\perp$ momenta. If the null subtraction removes the quadratic divergences correctly, the result for $F_1(q^2)+F_2(q^2)$ should be the same in both cases. We have checked this statement numerically [26]. Hence, the null subtraction restores the covariant answer also in the case of the $n=1$ jellyfish graph.

If we take those results, together with the fact that the one-loop Ward identities are satisfied for the good components in LCPT, one can say that the null subtraction preserves the Ward identities at one loop (for external fermion lines on shell).

It should also be mentioned that we have checked the null-subtraction method for the case of the two-loop rainbow self-energy in Fig. 5. More interesting, however, is the two-loop self-energy of Fig. 6 since it contains two $n=1$ jellyfish subdiagrams [27]. The corresponding null subtractions are

$$I_1=\frac{e^2}{(16\pi^3)^2}\int_0^1 d^2k_{1\perp}dx\int_0^{1-x}d^2k_{2\perp}dy\frac{1}{xy(1-x)(1-y)(1-x-y)}\times\frac{\gamma^\mu\frac{1}{2}\gamma^+\frac{\lambda^2+k_{1\perp}}{x}\gamma^-\frac{\lambda^2+k_{1\perp}^2}{x}\frac{1}{2}\frac{\gamma^+}{p^+}\gamma_\mu(\not p_2+m)\gamma_-}{\left[-\frac{m^2+k_{1\perp}^2}{1-x}-\frac{k_{1\perp}^2+\lambda^2}{x}\right]\left[-\frac{m^2+k_{1\perp}^2}{1-x-y}-\frac{k_{1\perp}^2+\lambda^2}{x}-\frac{\lambda^2}{y}\right]\left[p^--\frac{m^2+(p_\perp-k_{2\perp})^2}{1-y}-\frac{k_{2\perp}^2+\lambda^2}{y}\right]}, \tag{2.14}$$

where $p_2=(1-y,p^--(\lambda^2+k_{2\perp})/y,p_\perp-k_{2\perp})$ and

$$I_2=\frac{e^2}{(16\pi^3)^2}\int_0^1 d^2k_{1\perp}dx\int_0^{1-x}d^2k_{2\perp}dy\frac{1}{xy(1-x)(1-y)(1-x-y)}\times\frac{\gamma_-(\not p_1+m)\gamma_\mu\frac{\lambda^2+k_{2\perp}^2}{y}\frac{1}{2}\gamma^+\gamma^-\frac{\lambda^2+k_{2\perp}}{y}\frac{1}{2}\frac{\gamma^+}{p^+}\gamma^\mu}{\left[p^--\frac{m^2+(p_\perp-k_{1\perp})^2}{1-x}-\frac{\lambda^2+k_{1\perp}^2}{x}\right]\left[-\frac{m^2+k_{2\perp}^2}{1-x-y}-\frac{\lambda^2}{x}-\frac{\lambda^2+k_{2\perp}^2}{y}\right]\left[-\frac{m^2+k_{2\perp}^2}{1-y}-\frac{k_{2\perp}^2+\lambda^2}{y}\right]}, \tag{2.15}$$

respectively. Figure 6 shows the result of the numerical integration for different components. The result is that the null subtraction eliminates the quadratic divergence and restores a covariant form within the error of the calculation.

The general definition of the null subtraction of the n-photon jellyfish graph,

$$I_{J_n}=\frac{e^2}{(16\pi^3)}\int_0^{p^+}dk^+d^2k_\perp\frac{\Theta(p^+-k^+)\Theta(p^+-k^+-q_1^+)\cdots\Theta(p^+-k^+-\cdots-q_n^+)}{k^+(p^+-k^+)(p^+-k^+-q_1^+)\cdots(p^+-k^+-q_1^+-\cdots-q_n^+)}\times\frac{\gamma^\mu(\not p_1+m)\gamma^{\mu_1}(\not p_2+m)\gamma^{\mu_2}\cdots(\not p_n+m)\gamma_\mu}{\left[p^--k^--\frac{m^2+(p_\perp-k_\perp)^2}{P^+-k^+}\right]\cdots\left[p^--k^--\frac{m^2+(p_\perp-k_\perp-q_{1\perp}-\cdots-q_{n\perp})^2}{p^+-k^+-q_1^+\cdots-q_n^+}\right]}, \tag{2.16}$$

with external fermion momentum $p=(p^+,p^-,p_\perp)$ and momentum $q_i=(q_i^+,q_i^-,q_{i\perp})$ for the ith external photon line, is given by [28]

$$I^n_{\text{null}}=\frac{e^2}{(16\pi^3)}\int_0^{p^+}dk^+dk_\perp\frac{\Theta(p^+-k^+)\Theta(p^+-k^+-q_1^+)\cdots\Theta(p^+-k^+-\cdots-q_n^+)}{k^+(p^+-k^+)(p^+-k^+-q_1^+)\cdots(p^+-k^+-q_1^+-\cdots-q_n^+)}\times\frac{\gamma^\mu\frac{1}{2}p_1^-\gamma^+\gamma^{\mu_1}\frac{1}{2}p_2^-\gamma^+\gamma^{\mu_2}\cdots\frac{1}{2}p_n^-\gamma^+\gamma_\mu}{\left[\frac{-k_\perp^2+\lambda^2}{k^+}-\frac{k_\perp^2+\lambda^2}{p^+-k^+}\right]\left[\frac{-k_\perp^2+\lambda^2}{k^+}-\frac{k_\perp^2+\lambda^2}{p^+-k^+-q_1^+}\right]\cdots\left[\frac{-k_\perp^2+\lambda^2}{k^+}-\frac{k_\perp^2+\lambda^2}{p^+-k^+-q_1^+-q_2^+-\cdots-q_n^+}\right]}, \tag{2.17}$$

where $k^-=(k_\perp^2+\lambda^2)/k^+$. The fermion light-cone energies p_i^- are given by $p_i^-=-(k_\perp^2+\lambda^2)/k^+$, if p_i^- is set on energy shell, i.e., the ith fermion line does not extend over more than one intermediate state [14]. The on-mass-shell case yields $p_i^-=(m^2+k_\perp^2)/$

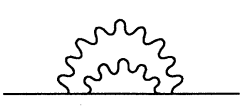

FIG. 5. Two-loop rainbow self-energy diagram.

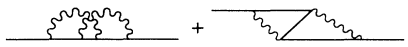

res.	component
-2656 ± 7.7	$\perp$
-2691 ± 37	+
-2641 ± 50	−

FIG. 6. The two-loop self-energy contribution of the electron is expected to be of the form $A+B\not{p}$, where p corresponds to the external fermion momentum. The result (res) shows the extraction of B by means of the various components of p.

$(p^+-k_1^+-q_1^+-\cdots q_i^+)$. Note that the null subtraction in (2.17) is to be used in combination with only one Pauli-Villars particle. Thus the number of degrees of freedom is considerably reduced. This was possible since all higher-loop noncovariant terms are independent of the photon mass.

The null subtraction was developed to deal consistently with quadratic divergences, in particular in the context of a numerical treatment.

III. LIGHT-CONE QUANTIZATION IN LIGHT-CONE GAUGE

For nonperturbative methods such as DLCQ or the lightfront Tamm-Dancoff procedure, $A^+=0$ gauge is by far the most favorable choice among all gauges. This is due to the fact that ghosts and spurious degrees of freedom should not occur in this case. Furthermore, it seems to be the only gauge where canonical light-cone quantization is tractable, since it avoids having the A^+ field in the denominator after solving the constraint equation for the left-handed spinors. In addition, only light-cone quantization in $A^+=0$ gauge provides a convenient extraction of hadronic structure functions and, therefore, ensures an intuitive picture of high-energy scattering processes. Because of our discussion of the previous section, we may add the fact that quadratic divergences and noncovariant terms are restricted to a much smaller set of diagrams, compared to any other gauge. However, as a noncovariant gauge, $A^+=0$ requires a careful regularization of its k^+ singularity, in particular because the covariant structure in a Hamiltonian formulation is already lost. Many procedures have been given in literature to regulate the light-cone gauge singularity [29–31]. In any event, every prescription gives rise to the introduction of a regularization parameter ϵ into the theory. It is essential for analytic, as well as numerical calculations, to ensure independence of physical quantities on the ϵ regulator.

In this section, we want to focus on ϵ prescriptions, which are easy enough to implement; i.e., they are of potential interest for practical applications in DCLQ or the light-front Tamm-Dancoff procedure. In addition, we investigate, in the particular example of the anomalous magnetic moment of the electron $(g-2)/2$, the sensitivity of physical observables to a truncation at finite ϵ. We start out with the light-cone gauge propagator, which has the form

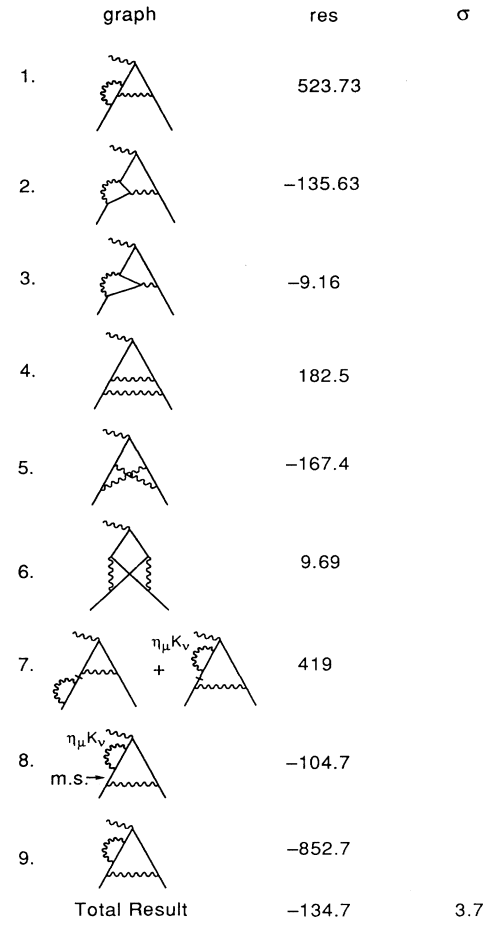

FIG. 7. Correction to e^+e^- scattering.

$$d_{\mu\nu}=-g_{\mu\nu}+\frac{\eta_\mu k_\nu+\eta_\nu k_\mu}{\eta\cdot k}\ , \tag{3.1}$$

where $\eta\cdot k\equiv k^+$ [32]. One possibility to regulate the $\eta\cdot k$ singularity is given by

$$d_{\mu\nu}=-g_{\mu\nu}+\frac{\eta_\mu k_\nu+\eta_\nu k_\mu}{\eta\cdot k}\Theta(\eta\cdot k-\epsilon)\ . \tag{3.2}$$

Note that the Θ function of the second term does not regulate the gauge piece only, but also all energy denominators which will multiply this term. Since gauge invariance in QED should occur locally (or quasilocally [34]), we expect the correct result for the anomalous magnetic moment of the electron for any value for ϵ between 0 and 1. This is exactly what we observe in our numerical calculations. It is instructive to see how the contributions of single diagrams add to the gauge-invariant answer. This is shown in Figs. 8 and 9. We remark that contributions of single diagrams grow logarithmically if ϵ gets small, which makes it more difficult to maintain the numerical accuracy for small values of ϵ. In order to obtain these results, it was essential to include the instantaneous self-energy diagram of Fig. 10, which vanishes in Feynman gauge. This is because the external self-energy diagram does contain a double pole in $A^+=0$.

	graph	res	σ	ε
1.		4941		0.05
2.		−172.9		
3.		2.34		
4.		−734.55		
5.		319.17		
6.	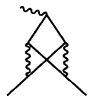	9		
7.	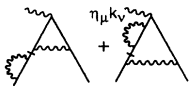	−121.1		
8.	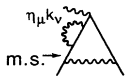	−3952		
9.		−428.8		
	Total Result	−137.8	5	

FIG. 8. Contributions (res) of single LCPT diagrams to the anomalous magnetic moment of the electron $a=(g-2)/2$ to fourth order in light-cone gauge for different values of the light-cone gauge cutoff ϵ. An ultraviolet cutoff $\Lambda=1000m$ was used, where m denotes the electron mass. The residual Λ dependence is within the error (σ) of the calculation. For convenience $\alpha/2\pi=10$ was chosen. m.s. associated with a line indicates that the corresponding fermion light-cone energy was taken on shell. $\eta_\mu k_\nu$ means that only the gauge piece of the corresponding photon propagator was used in this case.

The price we pay for the complete ϵ independence of physical observables for the regularization introduced in Eq. (3.2) is that for $\eta\cdot k<\epsilon$ the computation is carried out essentially in Feynman gauge. Indeed, we find

$$\eta_\mu d^{\mu\nu}(\epsilon)=-g^{+\nu}[1-\Theta(\eta\cdot k-\epsilon)]\neq 0 \tag{3.3}$$

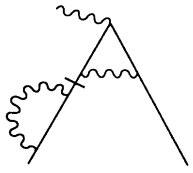

FIG. 9. Fourth-order correction to the electron anomaly in light-cone gauge for a different value of its gauge regulator. The analytic Feynman answer is given by -137.2 for $\alpha/2\pi=10$.

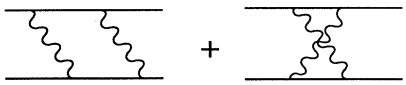

FIG. 10. Instantaneous contribution to the external wave-function correction in light-cone gauge.

for $\eta\cdot k<\epsilon$. Basically, any prescription which regulates the second term in Eq. (3.1) differently from the first one exhibits this feature. This is why, even in light-cone gauge, the existence of ghosts cannot be excluded in general [35]. From a technical point of view Eq. (3.2) means that the jellyfish problem does occur even in $A^+=0$ gauge. The only exception to this case is given by a regularization, introduced through

$$d_{\mu\nu}=\left[-g_{\mu\nu}+\frac{\eta_\mu k_\nu+\eta_\nu k_\mu}{\eta\cdot k}\right]\Theta(\eta\cdot k-\epsilon)\ , \tag{3.4}$$

which means that $A^+=0$ gauge is strictly obtained even at finite ϵ; i.e., $A^+(\epsilon)=0$. The advantage of this choice is the absence of ghosts and the jellyfish problem at finite ϵ. However, regularization (3.4) will, in general, truncate also physical contributions to Feynman integrals. Thus, correct physical answers are recovered only in the $\epsilon\to 0$ limit. For the purpose of practical applications, such as DLCQ, one can investigate the numerical significance of such a truncation. In Table I we present the result for the computation of $(g-2)/2$ for finite ϵ, using the prescription in Eq. (3.4).

IV. REGULATORS IN DLCQ

Nonperturbative methods should generally be compatible with perturbation theory in the weak-coupling domain of a theory. In lattice QCD, for example, the data scale as the one-loop β function for weak coupling. This important feature indicates the recovery of the correct continuum field theory for small values of the lattice spacing. A Hamiltonian formulation of field theory, such as DLCQ, should in principle reproduce correct perturbative results for any scattering process to finite order in the coupling. Thus, the calculation of $g-2$ to fourth order provides a powerful consistency check as well as an ideal testing ground for those methods.

We start our discussion with the test of the global cutoff, which is commonly used in DLCQ [33]. The global cutoff regulates an intermediate state with n particles

TABLE I. Total answer for the electron anomaly to fourth order in light-cone gauge for different values of the gauge regulator. The analytic Feynman answer is given by $a=-131.4\cdots(\alpha/\pi)^2$.

δa	ϵ
-128.3 ± 3.3	0.0
-125.6 ± 1.8	0.01
-105.3 ± 1.1	0.05
-57.5 ± 0.1	0.1

according to

$$\Theta\left[-\sum_{i=1}^{n}\frac{m_i^2+k_{i\perp}^2}{x_i}+\Lambda^2\right], \tag{4.1}$$

where $x_i, k_{i\perp}, m_i$ refer to the light cone x, the perpendicular momenta, and the mass of the ith particle, respectively. Λ denotes the ultraviolet cutoff, which is taken to infinity at the end of the calculation. Our result for the calculation of graph 1+2 in Fig. 1 is $R_{1+2}=(-0.34\pm0.005)\alpha^2/\pi^2$, which is to be compared with the analytic result by Petermann: $R_P=-0.3285\cdots\alpha^2/\pi^2$. The result for the ladder graph using the global cutoff is $(0.658\pm0.006)\alpha^2/\pi^2$. However, the correct answer is given by $R=0.778\alpha^2/\pi^2$. Thus, the global cutoff does not recover the correct continuum answer in the limit $\Lambda\to\infty$. Notice that there is no mass renormalization associated with the ladder diagram. Therefore, introducing "sector-dependent mass counterterms" (see, e.g., Ref. [3] for a discussion of the sector dependence of counterterms in the context of the Tamm-Dancoff approximation) does not help here either. In order to understand what has happened, we recall the Θ function in the $\mathbf{q}\to0$ limit for the counterterm (see graph 4 in Fig. 1):

$$\Theta\left[-\frac{m^2+k_{2\perp}^2}{1-x}-\frac{\lambda^2+k_{2\perp}^2}{x}+\Lambda^2\right], \tag{4.2}$$

where m,λ denote the fermion mass and the photon mass, respectively. Here, the variables $k_{2\perp}$ and x correspond to the loop momentum of the virtual photon [36]. However, the Θ function of the second intermediate state of the diagram corresponding to Fig. 13 is given by

$$\Theta\left[-\frac{m^2+(k_{2\perp}+k_{1\perp})^2}{1-x-y}-\frac{\lambda^2+k_{2\perp}^2}{y}-\frac{\lambda^2+k_{1\perp}^2}{x}+\Lambda^2\right]. \tag{4.3}$$

Obviously, (4.3) does not reduce to (4.2) in the large-$k_{2\perp}$ limit and hence does not allow a factorization of its infinite contribution. This effect induces the observed deviation from the correct answer in the $\Lambda\to\infty$ limit.

Recently, the so-called local cutoff has been proposed [37], which restricts the difference in the invariant mass locally, i.e., at a given vertex only, to values less than Λ^2/x. Here x is given by the fraction of the light-cone momentum which flows through the vertex under consideration. Hence, (4.3) gets replaced by

$$\left|-\frac{m^2+(k_{1\perp}+k_{2\perp})^2}{1-x-y}-\frac{\lambda^2+k_{2\perp}^2}{y}+\frac{m^2+k_{1\perp}^2}{1-x}\right|\leq\frac{\Lambda^2}{1-x}. \tag{4.4}$$

Changing variables according to $y=(1-x)\bar{y}$, $k_{2\perp}=\bar{k}_{2\perp}-\bar{y}k_{1\perp}$, and $\tilde{\Lambda}^2=\Lambda^2-m^2$ reduces (4.4) to (4.2) and, thus, avoids the problem of the global cutoff. Indeed, our calculations show that the local cutoff reproduces the correct result for the ladder graph. Unfortunately, it leads to the incorrect answer for graph 1+2 in Fig. 1. It is straightforward to show that the local cutoff violates gauge invariance already at the tree level [39].

Other Θ-function cutoffs that have been proposed [40] are also doomed to failure, unless a noncovariant counterterm is invoked. The reason is that they depend on momenta, i.e., derivatives only. However, a gauge-invariant regulator would require a functional dependence on covariant derivatives instead.

In Appendix C we demonstrate the implementation of dimensional regularization on the light cone.

V. SUMMARY

Light-cone quantization in Feynman gauge leads to an infinite number of quadratically divergent LCPT diagrams at the one-loop level. The problem occurs for self-energy diagrams where n photons ($n\geq0$) are inserted into the loop ("n-photon jellyfish problem"). We constructed a local representation of noncovariant counterterms, called the "null subtraction," in order to remove those divergences from the formalism.

In principle, also light-cone quantization in light-cone gauge exhibits this feature for all n (and not only for $n=0$). This is due to the fact that most regularizations of the light-cone gauge singularity reduce the small-x behavior of the photon propagator to that in Feynman gauge. In this case, the null subtraction can be used in the same way.

In Sec. III we evaluated the fourth-order correction to the anomalous magnetic moment of the electron in light-cone gauge and reproduced the analytic Feynman gauge result by Petermann. It was shown that a finite truncation of the $k^+\simeq0$ region can lead to a significant modification of the continuum result.

Finally, several ultraviolet cutoffs, which are commonly used in DLCQ, were tested in perturbation theory. It was shown that those regulators do not recover the correct continuum field theory in the $\Lambda\to\infty$ limit.

Appendix C demonstrates the introduction of dimensional regularization into the light-cone formalism.

ACKNOWLEDGMENTS

We gratefully acknowledge S. J. Brodsky for many useful comments on the paper. We would like to thank the Hoover Institution for its warm hospitality. This work was supported in part by the Department of Energy under contract DE-AC03-76SF00515. A.L. was supported in part by a grant from Studienstiftung des deutschen Volkes. M.B. was supported by the Alexander von Humboldt Foundation.

APPENDIX A

In this appendix we discuss the "method of alternate denominators," which was introduced in Ref. [14] as a possible way of removing quadratic divergences in the light-cone formulation. For illustration, the one-loop correction to the Compton graph, shown in Fig. 4, yields [41]

$$I_{\mathrm{Comp}}=\frac{\bar{u}\not{\epsilon}(\not{p}_1+m)}{p_1^+\left[p_i^- -\dfrac{m^2+p_{1\perp}^2}{p_1^+}\right]}\left[\int_0^{p^+}dk^+d^2k_\perp\frac{\gamma^\mu(\not{p}_1-\not{k}+m)\gamma_\mu}{(p_1-k)^+k^+\left[p_i^- -\dfrac{m^2+(p_\perp-k_\perp)^2}{p^+-k^+}-\dfrac{\lambda^2+k_\perp^2}{k^+}\right]}\right.$$
$$\left.-\int_0^{p^+}dk^+d^2k_\perp\frac{\gamma^\mu(\not{p}_1-\not{k}+m)\gamma_\mu}{(p_1-k)^+k^+\left[p_1^- -\dfrac{m^2+(p_\perp-k_\perp)^2}{p^+-k^+}-\dfrac{\lambda^2+k_\perp^2}{k^+}\right]}\right]$$
$$\times\frac{(\not{p}_1+m)\not{\epsilon}^*u}{p_1^+\left[p_i^- -\dfrac{m^2+p_{1\perp}^2}{p_1^+}\right]}\,. \tag{A1}$$

The second term is the alternate denominator (AD) subtraction, which is designed to cancel the quadratic divergence in the first term as well as perform the mass renormalization (see Fig. 11). The AD term is obtained by replacing the initial energy p_i^- in the energy denominator of the quadratically divergent subgraph by its adjacent energy p_1^- which is, in case of the self-energy diagram in Fig. 4, equal to the mass-shell energy $\tilde{p}_1^-$ (see below).

Obviously, the quadratic divergence is subtracted in this procedure since it is independent of the incoming energy. However, it remains to be shown that the mass subtraction of Fig. 11 is carried out correctly, using the AD method. Note that the AD term I_{AD} of Eq. (A1) is obtained by performing the k^- integration of

$$I_{\mathrm{AD}}=\int d^4k\frac{\bar{u}\not{\epsilon}(\not{p}_1+m)}{p_1^2-m^2+i\epsilon}\left[\frac{\gamma_\mu[(\tilde{\not{p}}_1-\not{k})+m]\gamma^\mu}{[(\tilde{p}_1-k)^2-m^2+i\epsilon]^2(k^2-\lambda^2+i\epsilon)}\right]\frac{(\not{p}_1+m)\not{\epsilon}^*u}{p_1^2-m^2+i\epsilon}\,. \tag{A2}$$

Here, $\tilde{p}_1$ is on shell, i.e., $\tilde{p}_1^\mu=p_1^\mu$ for $\mu\neq-$ and $\tilde{p}_1^-=(m^2+p_{1\perp}^2)/p_1^+$. However, the usual Feynman counterterm is given by

$$I_{\delta m}=\frac{1}{2m}\int d^4k\frac{\bar{u}\not{\epsilon}(\not{p}_1+m)}{p_1^2-m^2+i\epsilon}\left[\frac{\bar{u}(\tilde{p}_1)\gamma_\mu[(\tilde{\not{p}}_1-\not{k})+m]\gamma^\mu u(\tilde{p}_1)}{[(\tilde{p}_1-k)^2-m^2+i\epsilon]^2(k^2-\lambda^2+i\epsilon)}\right]\frac{(\not{p}_1+m)\not{\epsilon}^*u}{p_1^2-m^2+i\epsilon}\,. \tag{A3}$$

Obviously there is a difference between these two expressions because of the spinors $u(\tilde{p}_1)$ and $\bar{u}(\tilde{p}_1)$ which project out the δm piece from the self-energy in Eq. (A3). Thus, we conclude that the AD method must be used with caution. However, if one ignores the double instantaneous graph of Fig. 12 for a moment, at least one of the fermions is onshell, and the corresponding propagator

$$\frac{\not{p}_1+m}{p_1^2-m^2+i\epsilon}$$

gets replaced by

$$\frac{\tilde{\not{p}}_1+m}{p_1^2-m^2+i\epsilon}=\sum_s\frac{u(\tilde{p}_1,s)\bar{u}(\tilde{p}_1,s)}{p_1^2-m^2+i\epsilon}\,,$$

so that the missing projection onto the δm piece in Eq. (A3) is achieved by the adjacent on-shell fermion line. The point is that, unless one is cautious, the AD method treats the double instantaneous graph incorrectly by subtracting a nonzero contribution [42].

Thus, if one modifies the AD method such that the subtraction is excluded from the double instantaneous self-energy diagram, the usual (Feynman) answer can be obtained [43].

APPENDIX B

In this appendix we prove that the $n=0$ jellyfish graph (which is actually just the one-loop self-energy) with momentum $p=(p^+,p^-,p_\perp)$ has the form

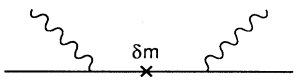

FIG. 11. Mass correction to electron Compton scattering.

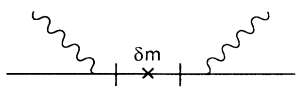

FIG. 12. Double instantaneous diagram to electron Compton scattering.

$$I_{n=0}=(\not{p}-m)B+(\not{p}-m)^2\Sigma(p^2)+\left[\frac{\gamma^+}{p^+}-\frac{\bar{u}\gamma^+u}{2mp^+}\right]C \tag{B1}$$

after mass renormalization. In the following we want to imply that the integral $\int d\lambda^2\rho(\lambda^2)=0$ is always taken; i.e., one Pauli-Villars subtraction is assumed. LCPT yields for the γ^- and $\gamma_\perp$ components for the $n=0$ jellyfish graph

$$\Sigma^{-,\perp}=-\frac{e^2}{16\pi^3}\int_0^1 dx\,d^2k_\perp\frac{\gamma^\mu(\not{p}-\not{k})\gamma_\mu}{(k_\perp-p_\perp x)^2-p_\perp^2x^2-p^-p^+x(1-x)+(m^2+p_\perp^2)x+\lambda^2(1-x)}\ , \tag{B2}$$

where the "good" vectors $\underline{p}=(p^+,0,p_\perp),\underline{k}=(k^+,0,k_\perp)$ have been introduced. The quantity x is given by the relative momentum carried by the virtual photon, i.e., $x=k^+/p^+$. Rewriting the denominator in terms of the four-momentum $p^2\equiv p^+p^--p_\perp^2$ and shifting integration variables yields

$$\Sigma^{-,\perp}=-\frac{e^2}{8\pi^3}\int_0^1 dx\,d^2k_\perp\frac{\not{p}(1-x)}{-k_\perp^2+x(1-x)p^2-m^2x-\lambda^2(1-x)}\ . \tag{B3}$$

For the γ^+ component we find

$$\Sigma^+=-\frac{e^2}{8\pi^3}\frac{1}{2}\frac{\gamma^+}{p^+}\int_0^1 dx\,d^2k_\perp\frac{(m^2+k_\perp^2)/(1-x)+p_\perp^2(1-x)}{-k_\perp^2+x(1-x)p^2-m^2x-\lambda^2(1-x)}\ . \tag{B4}$$

Since we are using Pauli-Villars regulator, the replacement $k_\perp^2\to p^2x(1-x)-m^2x-\lambda^2(1-x)$ does not change the value of the integral [44]. Thus,

$$\Sigma^+=-\frac{e^2}{8\pi^3}\frac{1}{2}\frac{\gamma^+}{p^+}\int_0^1 dx\,d^2k_\perp\frac{xp^2+m^2-\lambda^2+p_\perp^2(1-x)}{-k_\perp^2+x(1-x)p^2-m^2x-\lambda^2(1-x)}\ . \tag{B5}$$

Using

$$\begin{aligned}xp^2+(m^2-\lambda^2)&=-[(1-2x)p^2-m^2+\lambda^2]+(1-x)p^2\\&=-\frac{d}{dx}[p^2x(1-x)-xm^2-(1-x)\lambda^2-k_\perp^2]+(1-x)p^2\ ,\end{aligned}$$

we obtain

$$\begin{aligned}\Sigma^+=&\frac{e^2}{8\pi^3}\frac{1}{2}\frac{\gamma^+}{p^+}\int_0^1 d^2k_\perp dx\frac{d}{dx}\ln[p^2x(1-x)-xm^2-(1-x)\lambda^2-k_\perp^2]\\&-\frac{e^2}{8\pi^3}\frac{1}{2}\gamma^+\int_0^1 d^2k_\perp dx\frac{(1-x)p^-}{-k_\perp^2+x(1-x)p^2-m^2x+\lambda^2(1-x)}\ .\end{aligned} \tag{B6}$$

Obviously, the last integral corresponds to the integral in Eq. (B3) and is therefore part of the covariant answer. However, the first integrand in Eq. (B6) is noncovariant and leads to

$$C\frac{\gamma^+}{p^+}=\frac{e^2}{16\pi^3}\frac{\gamma^+}{p^+}\int d^2k_\perp\ln\frac{m^2+k_\perp^2}{\lambda^2+k_\perp^2}\ . \tag{B7}$$

The total answer becomes

$$\begin{aligned}\delta m+I_{n=0}=&\frac{e^2}{16\pi^3}\frac{\gamma^+}{p^+}\int_0^1 d^2k_\perp dx\frac{d}{dx}\ln[p^2x(1-x)-xm^2-(1-x)\lambda^2-k_\perp^2]\\&-\frac{e^2}{8\pi^3}\int_0^1 d^2k_\perp dx\frac{(1-x)(\not{p}-m)}{-k_\perp^2+x(1-x)p^2-m^2x-\lambda^2(1-x)}+\frac{-(1+x)m}{-k_\perp^2+x(1-x)p^2-m^2x-\lambda^2(1-x)}\ ,\end{aligned} \tag{B8}$$

where δm denotes the mass correction. Performing mass renormalization yields

$$\begin{aligned}I_{n=0}=&\frac{e^2}{16\pi^3}\left[\frac{\gamma^+}{p^+}-\frac{1}{2m}\bar{u}\frac{\gamma^+}{p^+}u\right]\int_0^1 d^2k_\perp dx\frac{d}{dx}\ln[p^2x(1-x)-xm^2-(1-x)\lambda^2-k_\perp^2]\\&-\frac{e^2}{8\pi^3}\int_0^1 d^2k_\perp dx\frac{(1-x)(\not{p}-m)}{-k_\perp^2+x(1-x)p^2-m^2x-\lambda^2(1-x)}\\&-\frac{e^2}{8\pi^3}\int_0^1 d^2k_\perp dx\frac{1}{-k_\perp^2+x(1-x)p^2-m^2x-\lambda^2(1-x)}\frac{(1-x^2)xm(p^2-m^2)}{-k_\perp^2+x(1-x)m^2-m^2x-\lambda^2(1-x)}\ .\end{aligned} \tag{B9}$$

Thus, we obtain the form of the self-energy in Eq. (C1).

APPENDIX C

In this appendix we demonstrate the use of dimensional regularization in light-cone quantization (see also Ref. [6]). For illustration we discuss the computation of the ladder diagram in Fig. 13. LCPT yields

$$F_L=\frac{e^4}{(16\pi^3)^2}\int_0^1 dx\,d^2k_1\int_0^{1-x}dy\,d^{2(1-\epsilon)}k_2\frac{1}{xy(1-x)^2(1-x-y)^2}$$
$$\times\frac{N(q,k_1,k_2)}{\left[m^2-\frac{m^2+k_1^2}{1-x}-\frac{k_1^2+\lambda^2}{x}\right]\left[m^2-\frac{m^2+(k_1+k_2)^2}{1-x-y}-\frac{k_1^2+\lambda^2}{x}-\frac{k_2^2+\lambda^2}{y}\right]},$$

where m,λ denote the fermion and photon mass, respectively. The Dirac numerator is abbreviated by $N(q,k_1,k_2)$ and will be specified later. Note, that the q dependence in the denominator can be dropped, in this particular example, since it gives no contribution to the anomaly. Notice further that only the inner loop is ultraviolet divergent and requires regularization. The introduction of dimensional regularization according to

$$\int dx\,d^2k\rightarrow\int dx\,d^{2(1-\epsilon)}k_\perp \tag{C1}$$

seems dangerous, particularly if the integrals are not absolutely convergent. However, (C1) is a direct consequence of the definition of dimensional regularization [45]. We have not yet encountered an example where (C1) leads to additional difficulties (in comparison to one Pauli-Villars photon and fermion, for example) in the light-cone formulation.

Shifting momenta and setting $m=1$ yields

$$F_L=\frac{e^4}{(16\pi^3)^2}\int_0^1 dx\,d^2k_1\int_0^1 dy\frac{y}{(1-x)^4x\,[1-(1+k_1^2)/(1-x)-k_1^-]^2}$$
$$\times\int d^{2(1-\epsilon)}\tilde{k}_2\frac{N(q,k_1,\tilde{k}_2-yk_1/(1-x))}{\left[\tilde{k}_2^2-\frac{y^2}{(1-x)^2}k_1^2+\frac{y(1-x-y)}{1-x}\left[-1+\frac{1+k_1^2}{1-x-y}+k_1^-+\frac{\lambda^2}{y}\right]\right]^2}, \tag{C2}$$

where $\tilde{k}_2=k_2+yk_1/(1-x)$ and $k_1^-=(k_1^2+\lambda^2)/x, k_2^-=(k_2^2+\lambda^2)/y$. If we expand the numerator according to

$$N(q,k_1,\tilde{k}_2-yk_1/(1-x))=A\tilde{k}_2^2+Bk_1+C\ , \tag{C3}$$

the last integration can be performed analytically by means of

$$\int\frac{d^{2\omega}l}{(2\pi)^{2\omega}}\frac{l_\mu l_\nu}{(l^2+M^2)^A}=\frac{1}{(4\pi)^\omega\Gamma(A)}\frac{1}{2}\delta_{\mu\nu}\frac{\Gamma(A-1-\omega)}{(M^2)^{A-1-\omega}}\ .$$

With the definition

$$f(k_1,x,y)=\frac{y}{(1-x)^4x}\frac{1}{\left[1-\frac{1+k_1^2}{1-x}-k_1^-\right]^2}\frac{1}{\frac{-y^2}{(1-x)^2}k_1^2+\frac{y(1-x-y)}{1-x}\left[-1+\frac{1+k_1^2}{1-x-y}+k_1^-+\frac{\lambda^2}{y}\right]},$$

one obtains

$$F_L=\frac{e^4}{(16\pi^3)^2}\int_0^1 d^2k_1\int_0^1 dy\,f(k_1,x,y)\left[(A+\epsilon A')\pi(1-\epsilon)\left[\frac{1}{\epsilon}-C_{\rm Eul}\right]+\pi(Bk_1+c)\right], \tag{C4}$$

where we have written $A(\epsilon)=A+\epsilon A'$. A, A', B can be computed using an algebraic manipulation program such as REDUCE. Equation (C4) can be integrated numerically. $C_{\rm Eul}$ is the Euler constant and given by $C_{\rm Eul}=0.577\cdots$.

The counterterm to Fig. 13 (see diagram 4 in Fig. 1) is computed in a similar way. It should be stressed that the pole in the one-loop vertex correction of diagram 4 in Fig. 1 not only cancels the pole in Eq. (C4) but also gives

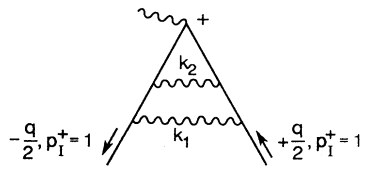

FIG. 13. Ladder diagram contribution to the electron anomaly in fourth order.

rise to a finite contribution [46].

We have redone the entire fourth-order calculation using dimensional regularization. Unlike the computation of the ladder graph, in general one has to combine energy denominators before the analytic part of the integration can be carried out. In contrast with a covariant theory, only one additional α parameter is necessary in light-cone quantization. This is due to the fact that the photon propagator $1/(k^2+i\epsilon)$ simply becomes $1/k^+$ in this case.

On the other hand, the coefficients A, A', B are harder to extract in light-cone quantization since the fermion energies generally depend implicitly on the loop momenta.

An understanding of dimensional regularization is essential, if one wants to extend LCPT to non-Abelian gauge theories.

[1] Stanley J. Brodsky, Nucl. Phys. **A544**, 223 (1992).

[2] T. Eller, H.-C. Pauli, and S. J. Brodsky, Phys. Rev. D **35**, 1493 (1987); K. Hornbostel, Ph.D. thesis, SLAC Report No. 0333, 1989; M. Burkardt, Nucl. Phys. **A504**, 762 (1989).

[3] A. Harindranath and R. J. Perry, Phys. Rev. D **43**, 492 (1991); R. J. Perry and A. Harindranath, *ibid.* **43**, 4051 (1991).

[4] We note that even (1+1)-dimensional theories, when quantized on the light cone, do not manifestly preserve parity. In fact, the fermion one-loop self-energy in the Yukawa model in 1+1 dimensions is logarithmically divergent, unless a careful regularization is imposed. This is due to the breakdown of parity, and in contrast with a covariant theory where the fermion self-energy is finite.

[5] By effective gauge invariance we mean that gauge invariance can be recovered in the continuum limit if a reasonable cutoff is introduced.

[6] D. Mustaki, S. Pinsky, J. Shigemitsu, and K. Wilson, Phys. Rev. D **43**, 3411 (1991).

[7] M. Burkardt and A. Langnau, Phys. Rev. D **44**, 3857 (1991).

[8] G. P. Lepage and S. J. Brodsky, Phys. Rev. D **22**, 2157 (1980).

[9] An alternative way of obtaining the different light-cone time orderings is by integrating out the light-cone energy of four-dimensional covariant Feynman diagram amplitudes.

[10] A. Langnau and S. J. Brodsky, J. Comput. Phys. (to be published).

[11] A. Petermann, Helv. Phys. Acta **30**, 407 (1957).

[12] C. M. Sommerfield, Ann. Phys. (N.Y.) **5**, 26 (1958).

[13] This is true with the exception of scalar electrodynamics, which also contains a quadratic divergence of the one-loop self-energy.

[14] S. J. Brodsky, R. Roskies, and R. Suaya, Phys. Rev. D **8**, 4574 (1973).

[15] This refers to the case where one always picks the $p_i^- \gamma^+$ component in the Dirac numerator for the fermion lines. In order to make the trace nonzero, all external photon lines must provide a γ^- vertex to the numerator. Thus, the problem does not occur in the $A^+=0$ gauge for $n \geq 1$.

[16] In the Feynman gauge those divergences cancel if all time orderings are summed. In the case of the light-cone gauge, those divergences cancel identically due to properties of the Dirac trace.

[17] In the particular example of $g-2$ to fourth order, the jellyfish problem for $n \geq 1$ does not occur if the spin-flip amplitude of the J^+ current is used for the extraction of the anomaly. This is due to the fact that γ^+ matrices cannot flip helicity.

[18] M. Burkardt and A. Langnau, Phys. Rev. D **44**, 1187 (1991).

[19] The tensor method can be used for the one-loop self-energy in the $A^+=0$ gauge as well, as long as the replacement (2.5) is restricted to the $g_{\mu\nu}$ piece in the propagator only.

[20] C. Bouchiat, P. Fayet, and N. Sourlas, Lett. Nuovo Cimento **4**, 9 (1972); S.-J. Chang and T.-M. Yan, Phys. Rev. D **7**, 1147 (1973).

[21] Unfortunately, we are not able to prove this rigorously. However, we have checked the most relevant two-loop diagrams to fourth order and verified the statement in these cases.

[22] F. J. Yndurain, *Quantum Chromodynamics* (Springer, New York, 1983), p. 210.

[23] This is provided the external fermion lines are on shell.

[24] In this case the null subtraction would subtract zero.

[25] Problems should not occur in this case since fermion light-cone energies do not contribute to the Dirac numerator because $\gamma^+\gamma^+=0$.

[26] As an example we cite the extraction of F_1+F_2 for the choice of the initial (in) and final (f) momentum given by $p_{\text{in}}=(0.4,4.3,0.85,0)$ and $p_{\text{f}}=(1,1,0,0)$. In the case of the good current we obtain $F_1+F_2=-250.1\pm1.3$. This is to be compared with $F_1+F_2=-248.5\pm1.5$. In this calculation we used a Pauli-Villars cutoff $\Lambda=10m$ and a photon mass $\lambda=10^{-4}m$, where m denotes the electron mass. For numerical reasons we chose $\alpha/2\pi=10$.

[27] It should be noted that no overlapping quadratic divergences occur in this example. This is because γ^- insertions are necessary at 2 and 3 in order to make both jellyfish diagrams quadratically divergent. However, this enforces γ^+ components at 1 and 4 (in the Feynman gauge), which leads to a zero result because only γ^+ components contribute to the fermion lines in this case. This result is consistent with the null subtraction.

[28] The case considered here involves incoming external photons only. If some of the photons are outgoing, the corresponding light-cone momenta q_i^+ must be set negative in (2.16).

[29] G. Leibbrandt, Rev. Mod. Phys. **59**, 1067 (1987).

[30] A. Basseto and R. Soldati, Phys. Rev. D **41**, 3277 (1990).

[31] O. Piguet, G. Pollak, and M. Schweda, Nucl. Phys. **B328**, 527 (1984).

[32] Note that the piece $\sim\eta_\mu\eta_\nu/(\eta\cdot k)^2$ is canceled in physical S-matrix elements by means of the instantaneous photon interaction. Effectively, instantaneous diagrams can be taken into account by putting those photon lines on energy shell which do not extend over more than one intermediate state. In order to avoid severe infrared problems, nonperturbative methods must include instantaneous con-

tributions if, and only if, the corresponding photon in flight contributes to the approximation [33].
[33] A. Tang, Ph.D. thesis, SLAC Report No. 351, 1990.
[34] In Fig. 7 a cancellation of the gauge piece in the propagator can be local for only one of the photons.
[35] This remark refers only to non-Abelian gauge theories.
[36] Note that the one-loop anomaly does not require regularization.
[37] S. J. Brodsky (private communication).
[38] Those violations of gauge invariance occur in all gauges, even if the so-called "gauge principle" is invoked [39].
[39] M. Kaluza and H. C. Pauli, Phys. Rev. D **45**, 2968 (1992).
[40] H. C. Pauli, M. Kaluza, and S. Brodsky (private communication).
[41] In order to regularize this expression, we want to assume that the Pauli-Villars condition $\int d\lambda^2 \rho(\lambda^2)=0$ has been imposed.
[42] The problem does not occur in the self-energy diagram 1 of Fig. 1 because the double instantaneous diagram does not contribute, since the J^+ current is computed here.
[43] In the light-cone gauge the situation is more complicated, due to extra terms of the form

$$\frac{\not\eta \not k(\not p - m)+(\not p - m)\not k \not\eta}{\eta k} + \frac{\not\eta (p^2-m^2)}{\eta k} .$$

We see that even single instantaneous graphs give rise to a mass subtraction in the AD method even though δm is gauge invariant.
[44] This is because the difference is independent of the photon mass.
[45] J. Collins, *Renormalization* (Cambridge University Press, Cambridge, England, 1984), p. 66.
[46] This is after multiplication with a term proportional to ϵ from the one-loop anomaly.